Probing O-H Bonding Through Proton Detected ^{1}H-^{17}O Double Resonance Solid-State NMR Spectroscopy

*Scott L. Carnahan[1,2], Bryan J. Lampkin[1], Pranjali Naik[1,2], Michael P. Hanrahan[1,2], Igor I. Slowing[1,2], Brett VanVeller[1], Gang Wu[3], Aaron J. Rossini[1,2]**

[1]*Iowa State University, Department of Chemistry, Ames, IA, USA 50011*

[2]*US DOE Ames Laboratory, Ames, Iowa, USA, 50011*

[3]*Department of Chemistry, Queen's University, Kingston, Ontario, Canada K7L 3N6*

AUTHOR INFORMATION

Corresponding Author

*e-mail: arossini@iastate.edu, phone: 515-294-8952.

ABSTRACT

The ubiquity of oxygen in organic, inorganic, and biological systems has stimulated the application and development of ^{17}O solid-state NMR spectroscopy as a probe of molecular structure and dynamics. Unfortunately, ^{17}O solid-state NMR experiments are often hindered by the combination of broad NMR signals and low sensitivity. Here, it is demonstrated that fast MAS and proton detection with the D-RINEPT pulse sequence can be generally applied to enhance the sensitivity and resolution of ^{17}O solid-state NMR experiments. Complete 2D $^{17}O \rightarrow {}^{1}H$ D-RINEPT correlation NMR spectra were typically obtained in fewer than 10 hours from less than 10 milligrams of material, with low to moderate ^{17}O enrichment (less than 20%). 2D ^{1}H-^{17}O correlation solid-state NMR spectra allow overlapping oxygen sites to be resolved on the basis of proton chemical shifts or by varying the mixing time used for ^{1}H-^{17}O magnetization transfer. In addition, *J*-resolved or separated local field (SLF) blocks can be incorporated into the D-RINEPT pulse sequence to allow direct measurement of one-bond ^{1}H-^{17}O scalar coupling constants ($^{1}J_{OH}$) or ^{1}H-^{17}O dipolar couplings (D_{OH}), respectively; the latter of which can be used to infer ^{1}H-^{17}O bond lengths. $^{1}J_{OH}$ and D_{OH} calculated from planewave density functional theory (DFT) show very good agreement with experimental values. Therefore, the 2D ^{1}H-^{17}O correlation experiments, ^{1}H-^{17}O scalar and dipolar couplings, and planewave DFT calculations provide a method to precisely determine proton positions relative to oxygen atoms. This capability opens new opportunities to probe interactions between oxygen and hydrogen in a variety of chemical systems.

INTRODUCTION

Oxygen is ubiquitous in organic, inorganic and biological systems, making it an intriguing element to study molecular structure and dynamics by ^{17}O solid-state nuclear magnetic resonance spectroscopy (SSNMR).[1-26] The ^{17}O nuclide has unfavorable NMR properties, however, including low natural isotopic abundance (~ 0.037%) and a gyromagnetic ratio that is approximately one-seventh that of ^{1}H. ^{17}O is also a half-integer quadrupolar nucleus with a nuclear spin (I) of 5/2 that often yields broad NMR powder patterns due to second-order quadrupolar broadening. The combination of broad NMR signals and low sensitivity often makes ^{17}O SSNMR experiments prohibitive. The most common approach to improving the sensitivity of ^{17}O NMR experiments is isotopic enrichment of oxygen-17, for which a variety of methods have been successfully demonstrated.[3, 27-31] More recently, it has been demonstrated that with the large NMR sensitivity enhancements provided by high-field dynamic nuclear polarization (DNP),[32-34] natural isotopic abundance ^{17}O NMR experiments can be performed on inorganic materials.[19, 23-24, 26, 35-36] The resolution of ^{17}O SSNMR spectra is most often improved either by utilizing selective ^{17}O labeling schemes,[37] working at the highest possible magnetic field strengths,[12, 25, 38-39] or using multiple quantum magic angle spinning (MQMAS).[2, 4, 14, 25, 40-41] Alternatively, heteronuclear correlation (HETCOR) spectra obtained with pulse sequences such as cross-polarization (CP), phase-shifted recoupling effects a smooth transfer of order (PRESTO), heteronuclear multiple quantum coherence (HMQC), transferred echo double resonance (TEDOR), etc., have been used to obtain 2D NMR spectra that correlate ^{17}O NMR signals to the high-resolution SSNMR signals from spin-1/2 nuclei such as ^{1}H, ^{13}C and ^{15}N.[4, 9, 11, 13, 16, 18, 20, 25] However, 2D HETCOR experiments and MQMAS experiments normally suffer from poor sensitivity and generally require very long experiment times, even on highly ^{17}O enriched materials.

In the past 20 years, fast magic angle spinning (MAS) and proton detection have been applied to enhance the sensitivity of SSNMR experiments with conventional spin-1/2 nuclei such as ^{13}C, ^{15}N, ^{29}Si, etc. With the exception of ^{14}N,[42] proton detection is not commonly applied to enhance the sensitivity of NMR experiments with quadrupolar nuclei. Proton detection in SSNMR is normally accomplished with CP; however, CP is generally very inefficient for half-integer quadrupolar nuclei such as ^{17}O.[43-45] Consequently, proton detection of quadrupolar nuclei is normally accomplished with dipolar-HMQC pulse sequences.[46] However, HMQC SSNMR experiments often have poor efficiency due to incomplete suppression of background ^{1}H NMR signals, t_1-noise, long ^{1}H longitudinal relaxation times (T_1) in the solid-state, and short ^{1}H transverse relaxation times (T_2). Recently, we have shown that the dipolar-refocused insensitive nuclei enhanced by polarization transfer (D-RINEPT)[46] is an efficient method to obtain proton detected 2D HETCOR SSNMR spectra of half-integer quadrupolar nuclei.[47] In a proton detected D-RINEPT experiment the quadrupolar spin is directly excited and then magnetization is transferred to the proton spins for detection. D-RINEPT is advantageous because it exploits the short T_1 relaxation times of the quadrupolar nucleus, unwanted ^{1}H signals can be suppressed by pre-saturation pulses, and quadrupolar signal enhancement schemes such as rotor assisted polarization transfer (RAPT)[48] can be directly incorporated. For example, we showed that it was possible to obtain a 2D ^{17}O→^{1}H D-RINEPT spectrum of histidine hydrochloride monohydrate with very low level ^{17}O enrichment (*ca*. 4%).[47]

Here, we demonstrate that fast MAS and proton detection with the D-RINEPT pulse sequence can be generally applied to enhance the sensitivity and resolution of ^{17}O SSNMR experiments on organic and inorganic materials. For organic solids, complete 2D ^{17}O→^{1}H D-RINEPT correlation NMR spectra can typically be obtained in a couple hours from less than 10

milligrams of material with low to moderate ^{17}O enrichment (less than 20%). The 2D ^{1}H-^{17}O correlation NMR spectra allow overlapping oxygen sites to be resolved on the basis of proton chemical shifts or by varying the mixing time for ^{1}H-^{17}O magnetization transfer. In addition, with fast MAS it is possible to measure one-bond ^{1}H-^{17}O scalar coupling constants ($^{1}J_{OH}$) as well as ^{1}H-^{17}O dipolar couplings (D_{OH}) which provide the O-H bond length. $^{1}J_{OH}$ and D_{OH} calculated from planewave density functional theory (DFT) show very good agreement with experimental results. Therefore, 2D ^{1}H-^{17}O correlation experiments, ^{1}H-^{17}O scalar and dipolar couplings, and planewave DFT calculations provide a method to precisely determine proton positions relative to oxygen atoms and probe bonding between oxygen and hydrogen in a variety of chemical systems.

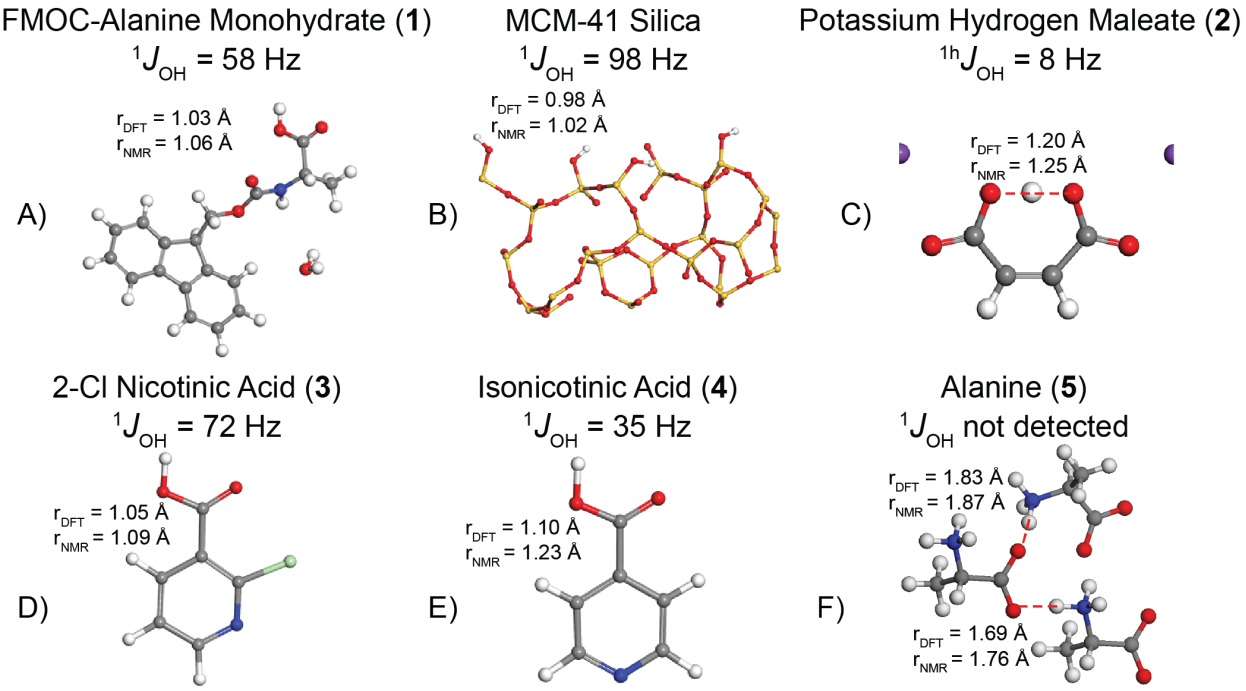

Chart 1. Structures of systems studied. The NMR determined O-H bond length (r_{NMR}) for MCM-41 silica is from reference [26]. DFT-optimized crystal structures are shown and the relevant crystal structure database (CSD) codes are included in Table S3. Red dashed lines show distance measurements that are not indicated by an O-H bond. See Results and Discussion for an explanation of bond length and scalar coupling measurements.

RESULTS AND DISCUSSION

Fast MAS ^{17}O Solid-State NMR Spectra of FMOC-Alanine Monohydrate. We begin with ^{17}O-enriched FMOC-alanine monohydrate (**1**) as a model sample (Chart 1). ^{17}O enrichment was performed with the multiple-turnover isotopic labeling method[29] with *ca*. 40% ^{17}O enriched water as the source. In this sample each carboxylate oxygen atom was enriched to *ca*. 19% ^{17}O abundance, as estimated using solution ^{17}O NMR spectroscopy (Figure S1).[49] The water of hydration in **1** was not ^{17}O-labeled since **1** was recrystallized from natural isotopic abundance H_2O. The ^{1}H and ^{17}O SSNMR spectra of **1** are shown in Figure 1. All NMR spectra in this study were obtained on a 1.3 mm double resonance probe with a 50 kHz MAS frequency, a main magnetic field of 9.4 T, and with RAPT for signal enhancement, unless otherwise indicated. For **1**, RAPT provided a 2.5-fold signal enhancement. The ^{17}O T_1 for **1** was measured to be 1.4 s with a saturation recovery experiment (Figure S2) and an optimal recycle delay of 2.0 s was used for all ^{17}O NMR experiments of **1**. The RAPT-enhanced ^{17}O spin echo NMR spectrum of **1** was obtained in 2.4 hours and has a signal-to-noise ratio (SNR) of *ca*. 12 (Figure 1A). A significant gain in sensitivity for ^{17}O detected experiments was obtained by using a RAPT-enhanced, rotor-synchronized quadrupolar Carr-Purcell-Meiboom-Gill (QCPMG) experiment[50] to obtain multiple spin echoes in each acquisition. An echo-reconstructed QCPMG spectrum was obtained in 2.5 hours and shows a SNR of 99 (Figure 1B), which corresponds to nearly an order of magnitude improvement in sensitivity compared to the spin echo spectrum. We note that for **1**, QCPMG is efficient because the ^{17}O effective transverse relaxation time constant (T_2') is relatively long (spin echoes can be acquired for *ca*. 40 ms). However, many of the other compounds we have examined have shorter ^{17}O T_2' values and QCPMG only provides limited gains in sensitivity.

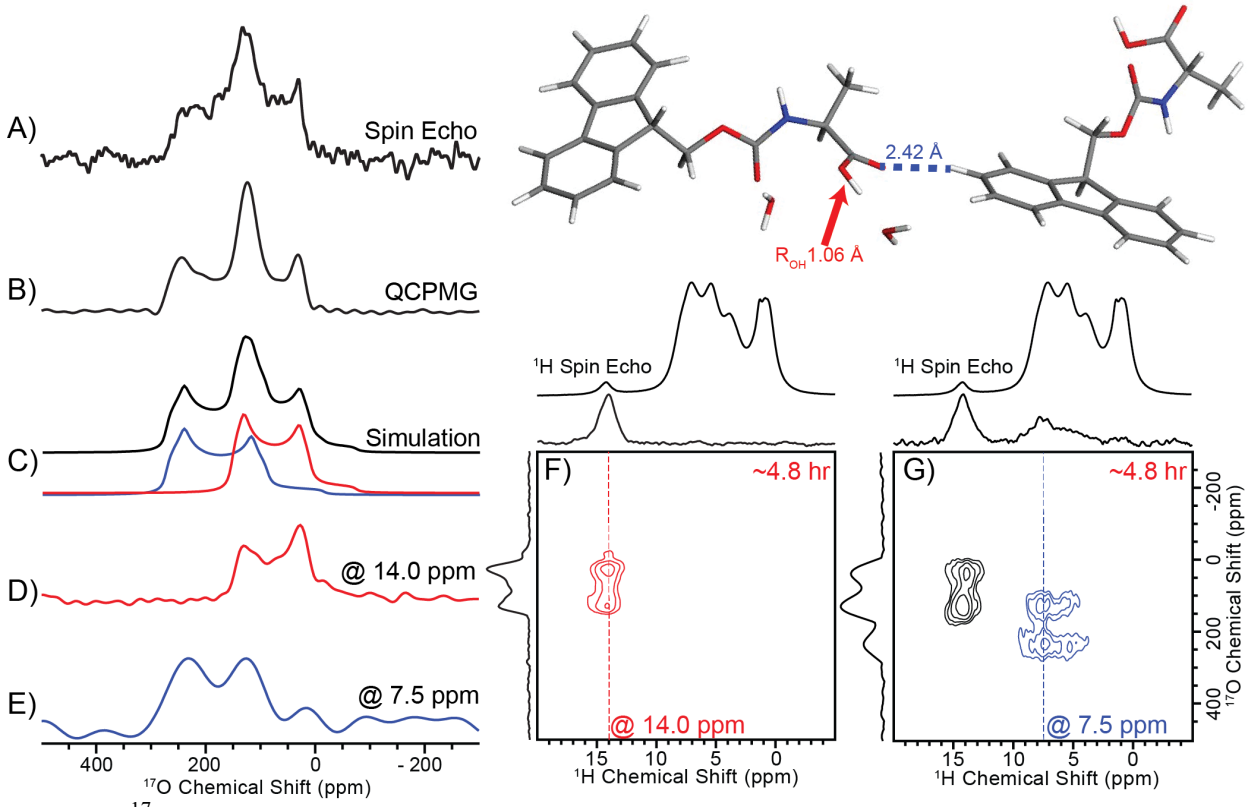

Figure 1. ^{17}O SSNMR spectra of compound **1** acquired with A) a spin echo, B) QCPMG, and (C) the corresponding two-site analytical simulation. ^{1}H detected ^{17}O D-RINEPT 2D SSNMR spectra with total recoupling times of (F) 160 μs and (G) 960 μs are shown on the bottom right. (D) and (E) Columns extracted from the 2D NMR spectra at ^{1}H chemical shifts indicated by the dashed lines. The geometry optimized single-crystal X-ray diffraction structure of **1** is shown in the upper right corner with key O-H distances indicated.

In agreement with the previously published ^{17}O solid-state NMR spectra of **1**,[7] the ^{17}O SSNMR spectrum consists of two overlapping ^{17}O NMR signals at the applied magnetic field of 9.4 T. The spectrum can be simulated with two sites (Figure 1C) and the ^{17}O NMR parameters determined here agree with those previously reported (Table 1). The site with the more positive isotropic chemical shift (δ_{iso} = 305 ppm) corresponds to the non-protonated carbonyl oxygen atom, while the site with δ_{iso} = 180 ppm corresponds to the oxygen atom of the carboxyl group that is bonded to the acidic proton.

Table 1. Summary of experimentally determined and calculated NMR parameters.

Sample		$\delta_{iso}(^{17}O)^a$	$\delta_{iso}(^{1}H)^a$	C_Q (MHz)	η_Q	$^{1}J_{OH}$ (Hz)	D_{OH} (kHz)	r_{OH} (Å)
FMOC-Alanine Monohydrate (**1**)	Site 1	173 (3)	14.3	7.1 (1)	0.18 (5)	58 (3)	13.5(5)	1.06(2)
	DFT	*187*	*13.1*	*-7.4*	*0.40*	*-55*	*-15.1*	*1.03*
	Site 2	305 (5)	7.7	7.9 (2)	0.18 (10)	-	-	-
	DFT	*339*	*6.6*	*-9.0*	*0.05*	*-*	*-*	*-*
MCM-41 Silica		1 (1)	1.8	3.1 (1)	0.30 (10)	98 (1)	-15.3[b]	1.02[b]
	DFT	*-3*	*5.3*	*-7.3*	*0.46*	*-90*	*-17.543*	*0.98*
KH Maleate (**2**)	Site 1	239 (5)	20.1	6.3 (2)	0.52 (10)	8 (23)	8.2(5)	1.25(3)
	DFT	*237*	*19.6*	*-6.3*	*0.59*	*-15*	*-9.371*	*1.20*
	Site 2	322 (4)	6.0	8.6 (1)	0.13 (5)	-	-	-
	DFT	*330*	*5.2*	*8.9*	*0.19*	*-*	*-*	*-*
2-Cl Nicotinic Acid (**3**)	Site 1	176 (3)	13.6	7.2 (1)	0.12 (5)	72 (3)	12.5(5)	1.09(2)
	DFT	*182*	*13.6*	*-7.4*	*0.10*	*-50*	*-14.238*	*1.05*
	Site 2	363 (3)	8.3	8.9 (2)	0.00 (10)	-	-	-
	DFT	*332*	*7.9*	*9.3*	*0.00*	*-*	*-*	*-*
Isonicotinic Acid (**4**)	Site 1	190 (3)	17.9	6.4 (2)	0.13 (10)	35 (7)	8.8(5)	1.23(2)
	DFT	*198*	*17.2*	*-6.9*	*0.19*	*-35*	*-12.209*	*1.11*
	Site 2	356 (6)	7.7	9.3 (2)	0.10 (5)	-	-	-
	DFT	*324*	*7.5*	*9.0*	*0.06*	*-*	*-*	*-*
L-Alanine (**5**)	Site 1	260 (10)	8.6	6.9 (4)	0.63 (25)	[c]	3.0(5)	1.76(10)
	DFT	*265*	*10.3*	*6.7*	*0.76*	*4*	*-3.392*	*1.69*
	Site 2	293 (7)	3.8	8.0 (2)	0.27 (20)	[c]	2.5(5)	1.87(10)
	DFT	*286*	*6.0*	*8.6*	*0.30*	*4*	*-2.676*	*1.83*

[a]Calculated values are shown in italics with δ_{iso} converted from chemical shielding values, σ_{iso}, using a correlation plot (Figures S3A and S3B). The dipolar coupling is abbreviated D_{OH}. [b]The experimental distance (r_{OH}) for MCM-41 silica is taken from reference [26]. [c]*J*-coupling not detected, but it is likely less than 8 Hz. For all parameters the uncertainty of the last digit(s) is given in parentheses.

Next, 2D proton detected $^{17}O \rightarrow {}^{1}H$ D-RINEPT NMR spectra of **1** were obtained (Figure 1F, G). The 2D proton-oxygen correlation NMR spectra of **1** allow overlapping oxygen sites to be resolved and experimentally confirms the oxygen NMR signal assignments. Simultaneously, proton detection also provides a substantial gain in sensitivity. For example, comparison of a 1D proton detected $^{17}O \rightarrow {}^{1}H$ D-RINEPT NMR spectrum yields sensitivity, S (S = SNR×time$^{-1/2}$), that is approximately 7 times greater than the spin echo spectrum and is the same as the QCPMG sensitivity (Figure S4 and Table S1). Consequently, a complete 2D proton-oxygen HETCOR SSNMR spectrum of **1** can be obtained with reasonable SNR in a similar experiment time as is required for the 1D spin echo or QCPMG NMR spectra. In comparison, the typical method for resolving overlapping ^{17}O SSNMR signals, MQMAS, inherently has a maximum sensitivity of 2/5 that of even the 1D spin echo.[40]

The 2D $^{17}O \rightarrow {}^{1}H$ D-RINEPT NMR spectrum acquired with a short total ^{1}H heteronuclear recoupling time of 160 μs shows a single correlation between the acid hydrogen atom (δ_{iso} = 14.0 ppm) and the protonated carboxylic acid oxygen atom (Figure 1F). This correlation clearly confirms the assignment of the protonated oxygen atom to the signal with a δ_{iso} of 180 ppm. A second 2D $^{17}O \rightarrow {}^{1}H$ D-RINEPT NMR spectrum was obtained with a total ^{1}H recoupling time of 960 μs (Figure 1G). This spectrum shows an additional correlation between hydrogen atoms with a chemical shift of *ca*. 7.5 ppm and the non-protonated, carbonyl oxygen of the carboxylic acid, which is consistent with the XRD structure.

In summary, the results obtained from **1** show that with proton detection it is possible to rapidly obtain 2D ^{17}O-^{1}H correlation SSNMR spectra. In addition to enhanced sensitivity, these experiments allow overlapping oxygen sites to be resolved and assigned by correlating the broad ^{17}O NMR signals to high resolution ^{1}H NMR signals. By varying the ^{1}H recoupling time in the D-

RINEPT experiment it is possible to identify oxygen sites that are close to or distant from hydrogen, allowing resonance assignments to be verified. However, it should be noted that ^{17}O sites further from protons have significantly lower polarization transfer efficiency under D-RINEPT due to proton relaxation under dipolar recoupling. As a consequence of the reduced sensitivity, it is difficult to obtain enough indirect dimension increments to avoid truncation broadening of the ^{17}O NMR signals from oxygen atoms without directly attached ^{1}H signals (for example, see Figure 1D). The truncation broadening leads to larger uncertainty in the EFG and chemical shift extracted from fits of the powder patterns.

Fast MAS ^{17}O Solid-State NMR Spectra of Other ^{17}O-Enriched Organic Solids. Fast MAS ^{17}O SSNMR experiments were performed on several other organic carboxylic acids: potassium hydrogen maleate (**2**), 2-Cl nicotinic acid (**3**), isonicotinic acid (**4**), and alanine (**5**) (Chart 1). In these samples the ^{17}O isotopic enrichment level of each carboxylic acid oxygen atom was between 15% and 20%. 1D spin echo and/or QCPMG NMR spectra and 2D D-RINEPT NMR spectra were obtained from all of these compounds (Figures S5–S8). Figure 2 shows the ^{17}O SSNMR spectra extracted from the columns of the $^{17}O \rightarrow {}^{1}H$ 2D D-RINEPT NMR spectra for the compounds studied. Each spectrum was obtained in total experiment times between 0.8 and 9 hours. Similar to **1**, all four of the compounds **2 - 5** had overlapping sites in their 1D ^{17}O solid-state NMR spectra. In all cases the overlapping sites could be resolved in the 2D D-RINEPT NMR spectra via correlations to different ^{1}H peaks. The ^{17}O SSNMR spectra obtained in this way also gave powder patterns that could be reasonably simulated with simple analytical simulations. However, in a couple of cases (Figure 2E, G) distorted and/or low signal to noise ratio ^{17}O powder patterns were obtained. As was previously mentioned, $^{17}O \rightarrow {}^{1}H$ coherence transfer may be inefficient for non-

protonated oxygen sites, leading to reduced sensitivity. Also, longer recoupling times are required to observe the ^{17}O NMR signals from the non-protonated (C=O) oxygen sites. Longer recoupling may cause the ^{1}H NMR signals to weakly correlate to more distant ^{17}O sites, leading to partial overlap of the ^{17}O NMR signals. But, since the protonated site can be clearly fit in the spectrum obtained from short recoupling time 2D NMR spectrum, the position of the discontinuities associated with the non-protonated site can be distinguished by process of elimination.

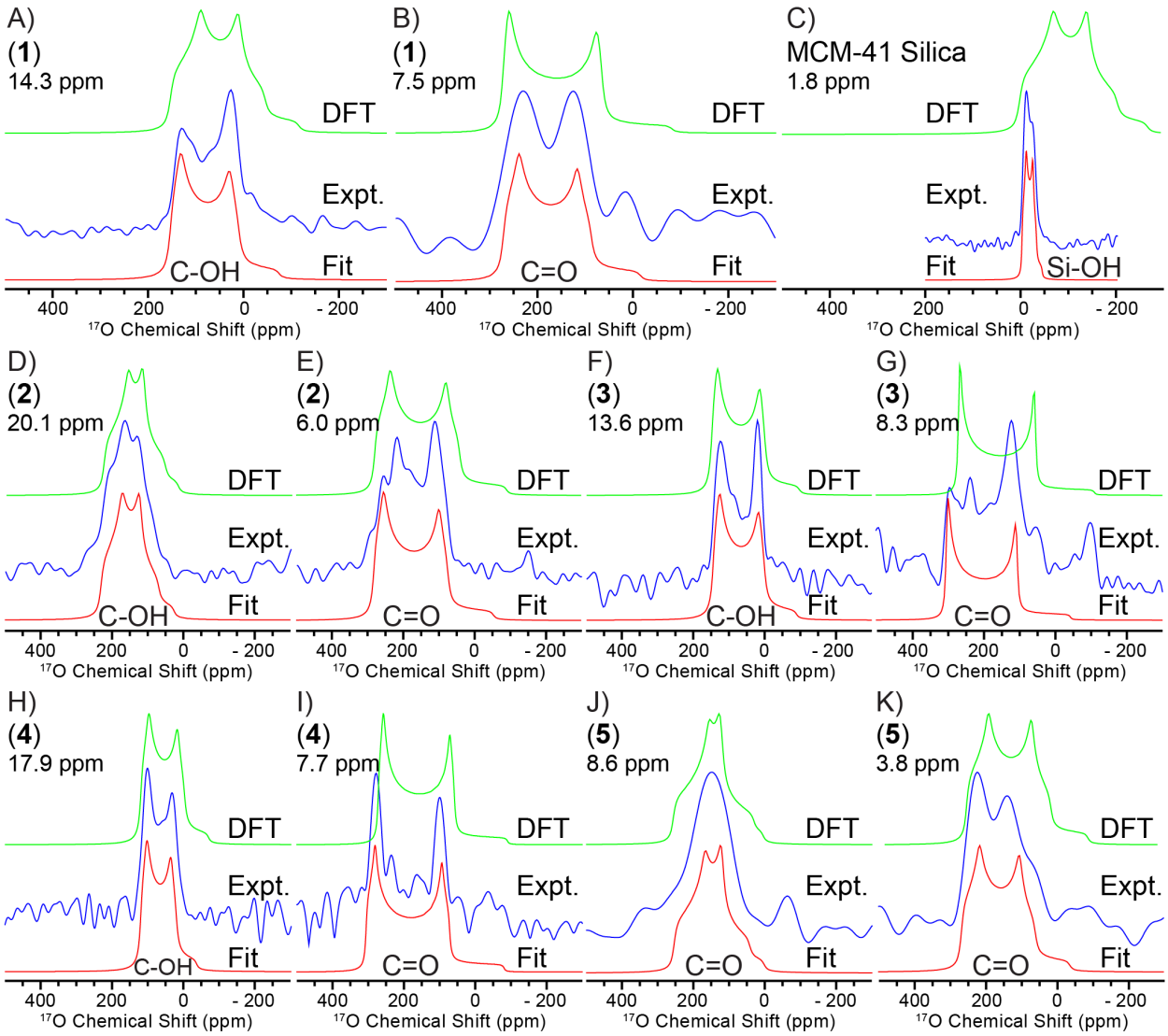

Figure 2. ^{17}O NMR spectra with (blue, middle) column slices from 2D $^{17}O \rightarrow {}^{1}H$ D-RINEPT spectra, (red, bottom) fits to the column slices, and (green, top) planewave DFT calculated spectra for A) FMOC-alanine monohydrate site 1, B) FMOC-alanine monohydrate site 2, C) MCM-41 silica, D) potassium hydrogen maleate site 1, E) potassium hydrogen maleate site 2, F) 2-Cl nicotinic acid site 1, G) 2-Cl nicotinic acid site 2, H) isonicotinic acid site 1, I) isonicotinic acid site 2, J) l-alanine site 1, and K) l-alanine site 2. The ^{1}H chemical shift of the column extracted from the 2D experiment is indicated. NMR parameters used for the fits and simulations with DFT predicted values are summarized in Table 1. The simulated spectra are processed with 400 Hz line broadening.

In general, 1D proton detected D-RINEPT NMR spectra provided 2 to 4 times higher sensitivity than QCPMG for these compounds with two notable exceptions (Table S1). For **4**, D-

RINEPT provided a ^{17}O NMR spectrum with 26 times better sensitivity than QCPMG. The large gain in sensitivity with proton detection was realized because the ^{17}O T_2' was very short in **4** and QCPMG had poor efficiency. For **5**, the 1D proton detected D-RINEPT NMR experiment had substantially worse sensitivity than the QCPMG experiment. This is likely because the ^{1}H-^{17}O dipolar coupling is small in **5** (*ca*. 3 kHz) which results in an inefficient ^{1}H-^{17}O coherence transfer and also because QCPMG provided particularly good efficiency in this sample. We note that many of these compounds have a very long ^{1}H T_1 (> 1 min), while the ^{17}O T_1 values ranged from 0.5 to 7 s (Table S2). Therefore, in many cases, D-RINEPT is likely to be the best method to obtain 2D correlation NMR spectra because the recycle delay is dictated by the shorter ^{17}O T_1 rather than the ^{1}H T_1. With methods such as HMQC, PRESTO, CP, etc., the proton spins will normally be excited first and the long ^{1}H T_1 will dictate the recycle delay of the experiment. In favorable cases, D-RINEPT can provide a slight gain in sensitivity as compared to QCPMG.

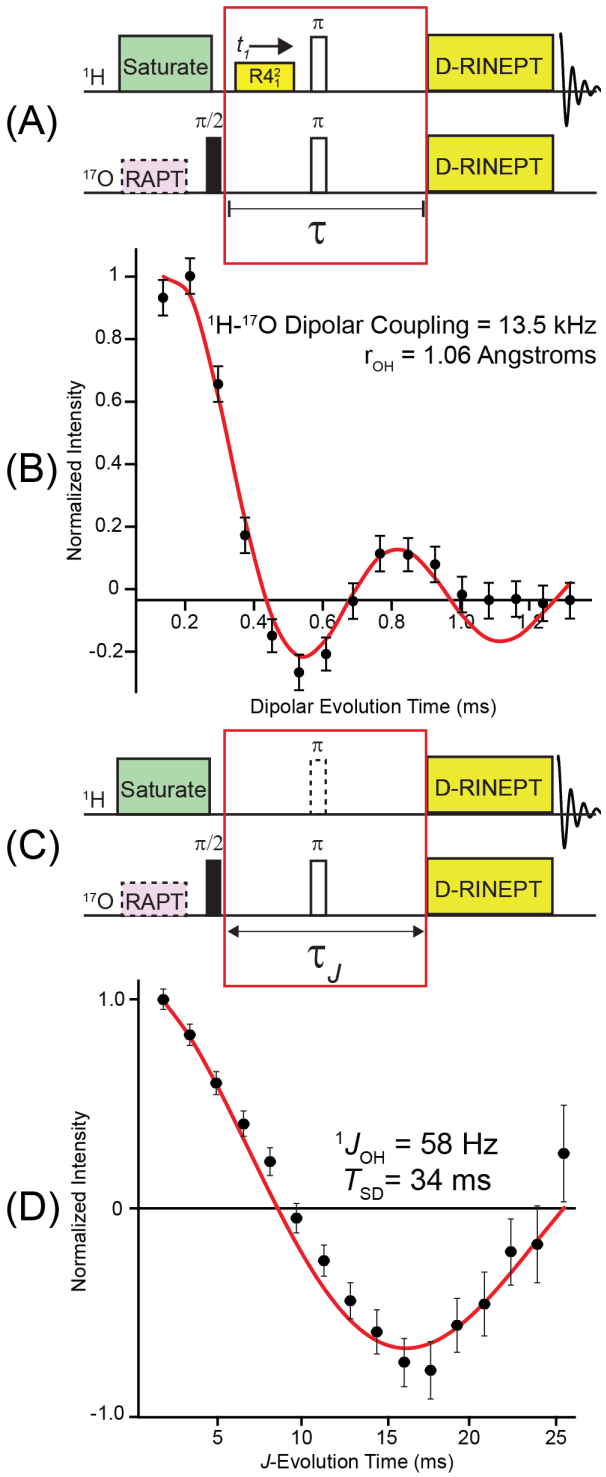

Figure 3. (A) Pulse sequence for a separated local field (SLF) D-RINEPT experiment used to measure ^{1}H-^{17}O dipolar couplings. (B) Dipolar dephasing curve for **1** (black points) and the best fit which corresponds to a 13.5 kHz ^{1}H-^{17}O dipolar coupling and a hydrogen-oxygen bond length of 1.06 Å. (C) Pulse sequence for *J*-resolved D-RINEPT with (D) *J*-dephasing curve for **1** fit to $^1J_{OH}$ = 58 Hz obtained with 50 kHz MAS. A description of the error fitting for (D) can be found in Figure S5. The spin diffusion correction term was T_{SD} = 34 ms (see Figure S14 and main text).

Measurement of ^{1}H-^{17}O Dipolar Couplings in FMOC-Alanine Monohydrate. It is straightforward to modify the D-RINEPT pulse sequence to measure ^{1}H-^{17}O dipolar couplings or scalar couplings (Figure 3). Dipolar couplings can be measured with symmetry-based recoupling separated local field (SLF) experiments.[51-52] Brinkmann and Kentgens, as well as Levitt, Dupree and co-workers have previously measured hydrogen-oxygen bond lengths with ^{17}O detected ^{1}H-^{17}O SLF experiments.[11, 53-54] In the proton detected SLF experiment a ^{17}O spin echo element of fixed duration is introduced at the beginning of the D-RINEPT pulse sequence. During the first half of the ^{17}O spin echo, a symmetry-based recoupling pulse sequence is applied to the ^{1}H spins and recouples heteronuclear dipolar couplings while suppressing homonuclear dipolar couplings (Figure 3A).[51-52] The duration of the recoupling scheme is incremented in a 2D experiment. Phase-alternated $\{R4_1^2\}_0\{R4_1^2\}_{180}$ was applied as the dipolar recoupling scheme on the ^{1}H channel.

The dipolar dephasing curve for **1** recorded with the proton detected D-RINEPT SLF pulse sequence is shown in Figure 3B. In this experiment, a short recoupling time was used in the D-RINEPT block and only the acidic proton of the carboxylic acid was observed in the direct dimension. Therefore, the dipolar oscillation curve only represents signal from the protonated oxygen atom. If required, a longer recoupling time could be used in the D-RINEPT block to record the dipolar oscillation curve for the non-protonated oxygen atom. The best simulation of the dipolar oscillation yields a proton-oxygen dipolar coupling constant of 13.5 kHz, which corresponds to a hydrogen-oxygen bond length of 1.06 Å. The simulated curves for several other dipolar coupling constants are shown in Figure S9 and summarized in Table S4. The numerical simulation takes into account the ^{17}O→^{1}H D-RINEPT magnetization transfer and the relative orientations of the Euler angles, which is important to obtain accurate dipolar coupling constants (see Figure S11). The single crystal X-ray diffraction (XRD) structure of **1** subjected to planewave

DFT geometry optimization exhibits a O-H bond length of 1.03 Å for the acidic proton. Since NMR is known to overestimate bond lengths by ~0.03 Å,[55] the measured value 1.06 Å can be considered to be in good agreement with the distance from planewave DFT/XRD (Table 1).[56]

Measurements of ^{1}H-^{17}O Dipolar Couplings in Other ^{17}O-Enriched Organic Solids. Fast MAS ^{1}H-^{17}O dipolar coupling measurements were performed on **2**, **3**, **4**, and **5**. The dipolar dephasing curves are shown in Figures S5-S8, respectively, and summarized in Table 1. The uncertainty in the measured ^{1}H-^{17}O dipolar coupling constants was estimated to be about ± 500 Hz based upon comparison of multiple simulated curves to the experimental curves (Figure S10, Table S4). The uncertainty in the dipolar coupling constants translates to uncertainties in the measured OH bond lengths on the order of 0.02 Å to 0.1 Å depending upon the magnitude of the ^{1}H-^{17}O dipolar coupling constant. The NMR measured values agree well with the bond lengths predicted by planewave DFT for all compounds (Figure S3D). The measured O-H distances are also in reasonable agreement with those obtained from neutron diffraction. Since neutron diffraction is uncommon, only **2** and **5** have known neutron diffraction structures. The neutron diffraction structure for **2** gives r_{OH} = 1.22 Å,[57] while SSNMR measured an r_{OH} = 1.25 Å and the DFT-optimized XRD structure gives r_{OH} = 1.20 Å. The neutron diffraction structure for **5** gives r_{OH} = 1.78 Å and 1.86 Å,[58] while SSNMR measured r_{OH} = 1.76 Å and 1.87 Å and the DFT-optimized XRD structure gives r_{OH} = 1.69 Å and 1.83 Å. Note that planewave DFT typically predicts O-H bond lengths that are ca. 0.02 Å longer than those measured by neutron diffraction.[59] It is well known that vibration/libration/motion causes SSNMR experiments to typically measure dipole coupling constants that correspond to bond lengths longer than those determined by neutron diffraction or planewave DFT.[11, 26, 51, 53-55]

Measurement of ^{1}H-^{17}O Scalar Couplings in FMOC-Alanine Monohydrate. Scalar couplings (*J*-couplings) result from electronic through-bond interactions and provide a direct probe of covalent bonding. There are very few previous measurements of $^{1}J_{OH}$ with solution ^{17}O NMR because ^{17}O self-decoupling[60] occurs due to rapid quadrupolar-induced ^{17}O longitudinal relaxation or ^{1}H chemical exchange of attached protons. $^{1}J_{OH}$ values of 89, 86, 84, and 79 Hz have previously been measured using ^{1}H solution NMR for dilute water,[61] methanol,[62] ethanol,[62] and salicylic acid,[63] respectively, dissolved in aprotic organic solvents. $^{17}O\{^{1}H\}$ *J*-HMQC SSNMR experiments were also used to measure a $^{1}J_{OH}$ of 107 Hz for the isolated surface silanol groups of heat treated silica,[18] which to the best of our knowledge is the only previous measurement of $^{1}J_{OH}$ in the solid-state. Autschbach and co-workers have previously applied DFT to calculate $^{1}J_{OH}$ in a variety of hydrogen bonded carboxylic acids.[64] They predicted that $^{1}J_{OH}$ ranged from 42 Hz to 99 Hz and showed that $^{1}J_{OH}$ was correlated to Wiberg bond indices (WBI) which quantify the bond order.[64]

Scalar couplings can be measured with a *J*-resolved[46, 65-66] block at the beginning of the D-RINEPT sequence (Figure 3C). The *J*-resolved D-RINEPT experiment is acquired in an interleaved manner where a reference spectrum is collected in the absence of a ^{1}H π-pulse during the ^{17}O spin echo, then a spectrum is recorded with a π-pulse applied on the ^{1}H channel (the 'dashed' π-pulse in Figure 3C) which results in a spectrum with the signal intensity modulated by the *J*-coupling.[67] The *J*-dephasing time (τ_J) is then increased in integer multiples of twice the rotor period. A normalized *J*-evolution curve free of transverse relaxation effects was obtained by comparing the intensity of the reference spectrum to the *J*-dephased spectrum for each time point (Figure 3D).[67] The complete *J*-resolved data set for **1** is shown in the SI (Figure S13). A precisely set magic angle (approximately within 0.02 degrees) is necessary to completely average the contribution due to the dipolar coupling and obtain a pure *J*-dephased curve (Figure S14).[68] It was

straightforward to set the magic angle to within 0.01 degrees accuracy by minimizing the splitting in the ^{2}H spectrum of deuterated oxalic acid due to the first order quadrupolar interaction.[69]

In addition to accurate setting of the magic angle, ^{1}H spin diffusion must be suppressed in order to allow the coherent evolution of *J*-couplings in the solid-state.[70-71] Spin diffusion rates depend upon both the dipolar coupling between two spins and the peak overlap integral.[72] Therefore, narrowing of the ^{1}H peaks either by application of homonuclear decoupling and/or fast MAS also helps to suppress ^{1}H spin diffusion.[70-71] For the organic solids studied here, the ^{1}H NMR signals of the protons attached to oxygen are generally well resolved from the other ^{1}H NMR signals, which helps to reduce the spin diffusion rate,[72] making *J*-resolved NMR experiments feasible without application of homonuclear decoupling. For example, the ^{1}H T_1 values are distinct for the acid proton and other protons under 50 kHz MAS for **1**, suggesting that ^{1}H spin diffusion has been partially slowed (Table S2). However, 2D spin diffusion ^{1}H-^{1}H correlation spectra show that the acid ^{1}H peak exchanges magnetization with other ^{1}H spins on a similar timescale as the *J*-coupling evolution (Figure S15). Therefore, an additional phenomenological damping exponential decay term (T_{SD}) was added into the function used for fitting of the transverse-relaxation normalized *J*-resolved curves:

$$S(\tau_J) = A * \cos(\pi * J * \tau_J) * \exp\left(\frac{-\tau_J}{T_{SD}}\right).$$

Here, A is a scalar to adjust the intensity ($A \approx 1.0$ in all cases), J is the $^{1}J_{OH}$ coupling, and τ_J is the *J*-evolution time. The *J*-dephasing curve for **1** acquired with the proton detected *J*-resolved D-RINEPT pulse sequence is shown in Figure 3D. The experimental *J*-resolved curves and fits are shown in the SI for all other compounds. A fit of the experimental *J*-resolved curve for **1** yields $^{1}J_{OH}$ = 58 Hz and T_{SD} = 34 ms. The T_{SD} value of 34 ms is similar to the spin diffusion time constant of 30 ms measured with 2D spin diffusion NMR experiments on **1** at 60 kHz MAS, confirming

that the damping of the *J*-resolved curve is related to ^{1}H spin diffusion (Figure S15). For the other compounds, T_{SD} was measured to be between 15 and 60 ms. In general, for compounds with a substantial $^{1}J_{OH}$ (> 30 Hz) the fits of the *J*-resolved curves with and without damping yield similar $^{1}J_{OH}$. However, for smaller $^{1}J_{OH}$ the damping must be taken into account when fitting the *J*-resolved curves as it will make a significant contribution to the observed dephasing.

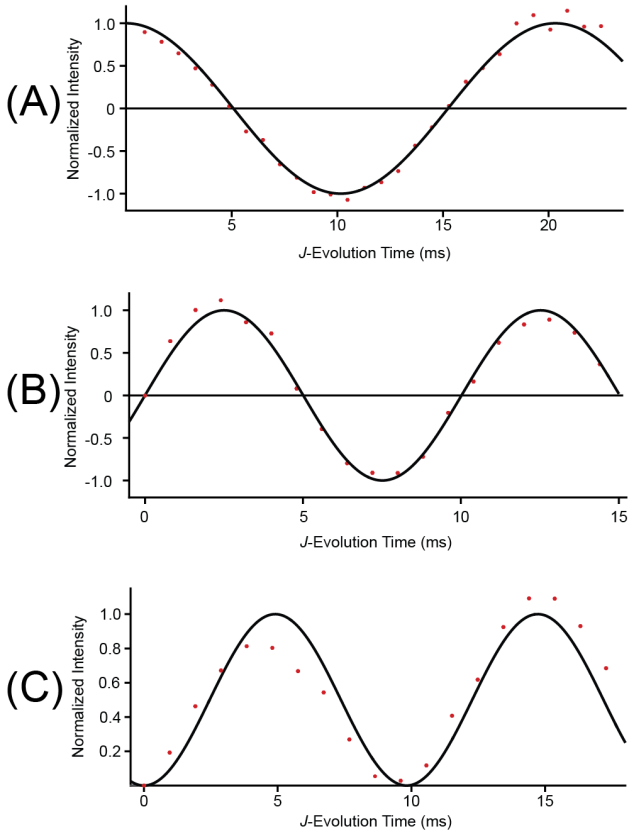

Figure 4. *J*-modulated curves for isolated silanol group on MCM-41 silica measured using (A) *J*-resolved D-RINEPT (Figure 3C), (B) *J*-RINEPT (Figure S16F), and (C) *J*-HMQC (Figure S16G). The $^{1}J_{OH}$ were fit to 98, 100, and 102 Hz, respectively. Experimental data points are shown as red circles and black lines correspond to fits to ideal functions. The *J*-RINEPT and *J*-HMQC curves were fit to the functions $S(\tau) = \sin(2\pi * J * \tau_J)$ and $S(\tau) = \sin^2(2\pi * J * \tau_J)$, respectively.

Measurements of $^{1}J_{OH}$ for MCM-41 Silica. In order to confirm the validity of our methods we measured the $^{1}J_{OH}$ for isolated silanols on the surface of silica, for which the only value of $^{1}J_{OH}$ in the solid state is known (107 Hz).[18] Silica is also a good test compound for these experiments

because the isolated surface silanols have long ^{17}O T_2 and ^{1}H T_2, each about 15 ms. The long ^{1}H T_2 likely arises because the hydroxyl groups are isolated on the silica surface. Given the long ^{17}O and ^{1}H transverse relaxation times, $^{1}J_{OH}$ was able to be measured for silica using three different pulse sequences, *J*-resolved D-RINEPT, *J*-RINEPT, and *J*-HMQC, which all produced *J*-coupling values *ca*. 100 Hz (Figure 4A-C). The slight deviation from the previous measurement of $^{1}J_{OH}$ in silica may exist because a different type of silica was studied and the strength of the O-H bond depends on hydration.[73-74] The long ^{1}H T_2 and absence of spin diffusion-induced damping in all of the *J*-based signal evolution curves confirms that the hydroxyl groups are isolated on the surface and do not undergo fast ^{1}H spin diffusion.

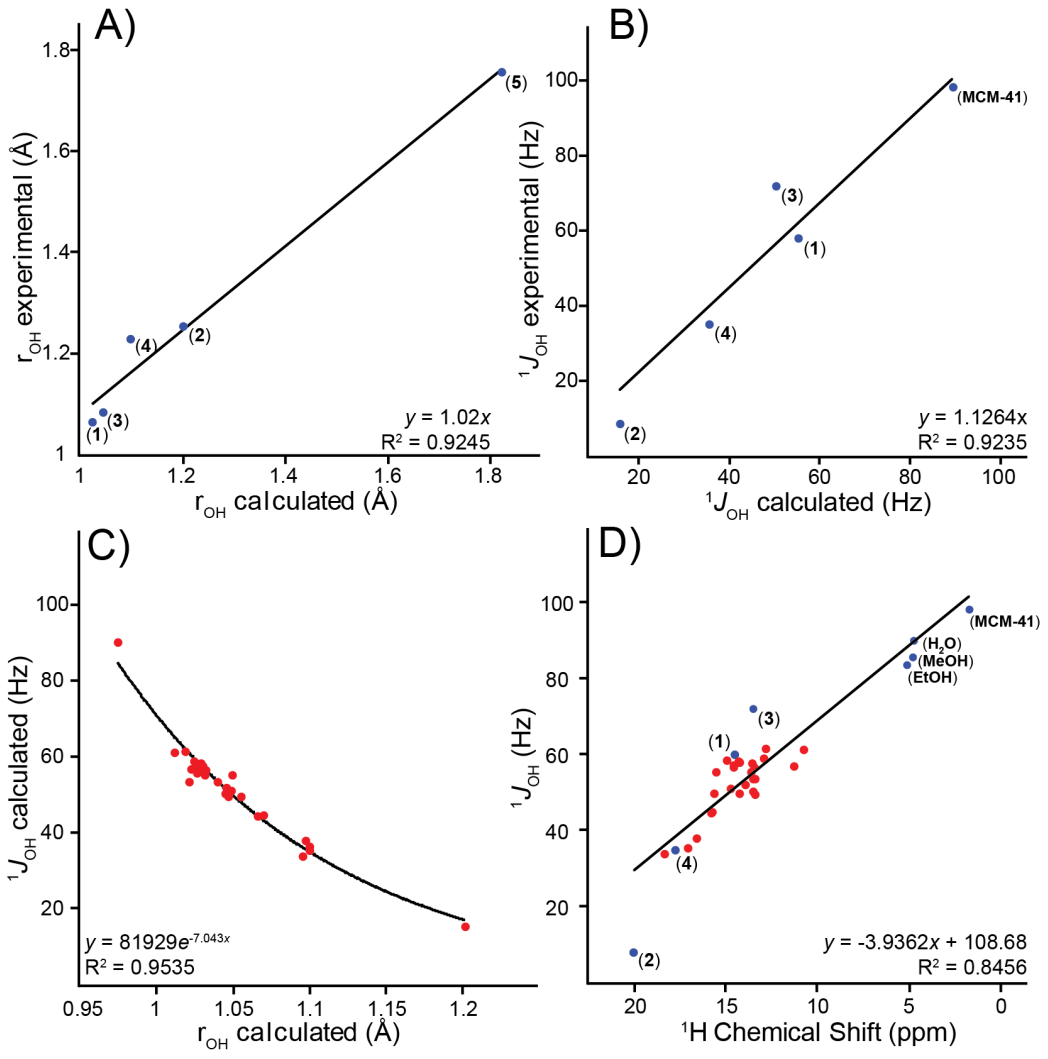

Figure 5. Comparison of experimental and calculated (A) O-H bond lengths and (B) *J*-couplings. Correlation of experimental and calculated *J*-couplings to (C) O-H bond length and to (D) the ^{1}H chemical shift of the attached proton. In plots (B-D) only the magnitude of $^{1}J_{OH}$ is considered. (D) includes the experimental solution-state values from references [61] and [62]. Experimental values are blue and calculated values are red. In (C) and (D) calculated *J*-couplings are shown for 25 additional compounds (see Chart S1 and Table S6 for the list of compounds).

Measurements of $^{1}J_{OH}$ for Other Organic Solids. The set of compounds studied here (Chart 1) represents a variety of oxygen-hydrogen interactions, including strong covalent silanol O-H bonds, weaker O-H bonds in carboxylic acids, and a hydrogen-bonded system (denoted $^{1h}J_{OH}$). The samples have O-H bond lengths ranging from 1.02 Å – 1.76 Å and there is a correspondingly large distribution in the measured $^{1}J_{OH}$, which range from 98 to 8 Hz. These systems were also studied by planewave DFT calculations (Table 1). The computed values for the O-H bond length and the $^{1}J_{OH}$ values are in good agreement with those measured experimentally (Figure 5A, B), with the exception of **3** for which the $^{1}J_{OH}$ was underestimated by DFT by about 20 Hz.

J-resolved experiments were attempted on para-toluene sulfonic acid monohydrate (PTSA) and calcium hydroxide ($Ca(OH)_2$) and ^{17}O NMR spectra were acquired for both samples (Figure S19 and Table S10). However, it was not possible to measure $^{1}J_{OH}$ in either compound. The hydronium ion in PTSA had a very short ^{17}O T_2, which prevented measurement of $^{1}J_{OH}$. $Ca(OH)_2$ also showed a short ^{17}O T_2 in the *J*-resolved experiments; but, the ^{17}O T_2 was quite long in QCPMG experiments. The rapid dephasing in the *J*-resolved experiment likely occurs because of rapid ^{1}H spin diffusion amongst the strongly dipolar-coupled hydroxide protons in the lattice, which all resonate with the same isotropic ^{1}H chemical shift. Both these cases have possible solutions which we can't yet implement in our lab. PTSA could be cooled to lower temperatures to extend the ^{17}O T_2. Faster MAS rates, partial deuteration, and/or homonuclear decoupling could slow ^{1}H spin diffusion and allow measurement of $^{1}J_{OH}$ in $Ca(OH)_2$.

Planewave DFT Calculation of ^{17}O NMR Parameters. In order to elucidate trends related to O-H bonding, DFT calculations were performed on all of the compounds in Chart 1 (Table 1). Additionally, in order to confirm relationships between O-H bond length and $^{1}J_{OH}$ calculations were performed on a set of 25 nicotinic acid derivatives with known crystal structures (Chart S1 and Table S6). As expected, planewave DFT accurately calculates ^{17}O chemical shifts and the quadrupolar coupling constant (C_Q) for all of the compounds in Chart 1 except for MCM-41 silica.[75] It has previously been demonstrated by ^{2}H and ^{17}O solid-state NMR experiments that the silanol groups on silica are dynamic.[36, 76] Therefore, the experimental ^{17}O lineshape of MCM-41 silica was most likely narrowed due to partial averaging of the ^{17}O electric field gradient (EFG), which explains the large discrepancy between experimental and calculated ^{17}O C_Q. Calculations of the C_Q were qualitatively correct (Figure S3E) but were systematically overestimated by DFT, which is a known phenomenon.[77] An exponential correlation between the geometry optimized O-H bond lengths and the *J*-coupling value was found (Figure 5C). This exponential relationship between bond length and *J*-coupling is similar to that reported for $^{1}J_{CC}$,[78] $^{2}J_{PH}$,[79] $^{3}J_{PN}$,[79] and $^{3}J_{CN}$.[80] A significantly positive ^{1}H chemical shift usually indicates that the O-H group is involved in strong hydrogen bonding thus weakening the covalent O-H bond. As expected, the magnitude of the $^{1}J_{OH}$ coupling decreases with increasing ^{1}H chemical shift for the O-H groups (Figure 5D).

CONCLUSIONS

In conclusion, we have shown that 2D ^{1}H-^{17}O correlation spectra can be rapidly acquired using proton detection, fast MAS, and the D-RINEPT pulse sequence. Notably, with small diameter 1.3 mm rotors these experiments require only a few mg of material and moderate ^{17}O enrichment. The 2D ^{1}H-^{17}O correlation spectra allow overlapping oxygen signals to be resolved

on the basis of the correlated ^{1}H chemical shifts. One-bond ^{1}H-^{17}O scalar coupling constants and ^{1}H-^{17}O dipolar coupling constants were also measured and provide a direct measure of the O-H bond strengths and lengths. The magnitude of the *J*-coupling directly gives insight into the type of O-H bond, *i.e*. alcohol, acid, or hydrogen bond.[64] The experimentally determined scalar and dipolar coupling constants were accurately predicted by planewave DFT calculations. $^{1}J_{OH}$ was calculated for a further set of 25 compounds to explore trends in the *J*-coupling as related to bond length and ^{1}H chemical shift. Continued advances in ^{17}O NMR, including measurement and prediction of $^{1}J_{OH}$ and O-H bond lengths, will give insight into O-H covalent and hydrogen bonding in numerous fields including pharmaceuticals, biological systems, and acid catalysts.

One challenge associated with ^{17}O SSNMR spectroscopy is that labeling can be time intensive and expensive; however, mechanochemistry methods have shown promise to improve the efficiency, cost, and ease of ^{17}O labeling.[31] With respect to the cost of ^{17}O-enriched samples, fast MAS rotors are beneficial because they typically require less than 10 mg of material. Alternatively, DNP-enhanced ^{17}O SSNMR could potentially be applied to allow these measurements on natural abundance samples.[23, 26, 35-36] We also anticipate that double resonance ^{1}H-^{17}O SSNMR experiments will benefit from higher magnetic fields and faster MAS rates, both of which will help to reduce ^{1}H spin diffusion rates and improve ^{1}H resolution. High magnetic fields will generally improve sensitivity and enhance resolution by increasing ^{1}H peak dispersion and narrowing ^{17}O peaks broadened by the 2nd order quadrupole interaction.[25]

Graphical Abstract

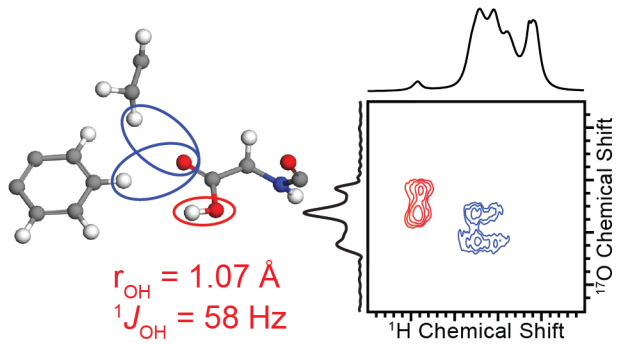

SUPPORTING INFORMATION

The Supporting Information contains the experimental section, additional solid-state NMR spectra, discussions of sensitivity enhancements from proton detection, experimental parameters, DFT calculated values, and pulse sequences.

ACKNOWLEDGMENT

This material is primarily based upon work supported by the National Science Foundation under Grant No. 1709972 to AJR. Any opinions, findings, and conclusions or recommendations expressed in this material are those of the author(s) and do not necessarily reflect the views of the National Science Foundation. AJR also thanks Iowa State University and the Ames Laboratory (Royalty Account) for additional support. PN and IIS thank support from the U.S. Department of Energy, Office of Basic Energy Sciences, Division of Chemical Sciences, Geosciences and Biosciences through the Ames Laboratory. The Ames Laboratory is operated for the U.S. DOE by Iowa State University under contract no. DE-AC02-07CH11358. GW thanks NSERC of Canada for funding. We thank Mr. Amrit Venkatesh, Ms. Rachel E. Gloeckner, and Mr. Matthew J. Ryan for assistance packing rotors and running NMR experiments.

REFERENCES

1. Schramm, S.; Kirkpatrick, R. J.; Oldfield, E., Observation of High-Resolution Oxygen-17 NMR Spectra of Inorganic Solids. *J. Am. Chem. Soc.* **1983,** *105*, 2483-2485.
2. Wu, G.; Rovnyak, D.; Huang, P. C.; Griffin, R. G., High-Resolution Oxygen-17 NMR Spectroscopy of Solids by Multiple-Quantum Magic-Angle-Spinning. *Chem Phys Lett* **1997,** *277* (1-3), 79-83.
3. MacKenzie, K. J. D.; Smith, M. E., *Multinuclear Solid-State NMR of Inorganic Materials*. Pergamon: 2002; Vol. 6.
4. Readman, J. E.; Kim, N.; Ziliox, M.; Grey, C. P., 17O MQMAS NMR Studies of Na-A and Ca-A. *Chem. Commun.* **2002,** (23), 2808-2809.
5. Wu, G.; Dong, S.; Ida, R.; Reen, N., A Solid-State 17O Nuclear Magnetic Resonance Study of Nucleic Acid Bases. *J. Am. Chem. Soc.* **2002,** *124* (8), 1768-1777.
6. Lemaitre, V.; Smith, M. E.; Watts, A., A Review of Oxygen-17 Solid-State NMR of Organic Materials-Towards Biological Applications. *Solid State Nucl. Magn. Reson.* **2004,** *26* (3-4), 215-235.
7. Pike, K. J.; Lemaitre, V.; Kukol, A.; Anupold, T.; Samoson, A.; Howes, A. P.; Watts, A.; Smith, M. E.; Dupree, R., Solid-State 17O NMR of Amino Acids. *J. Phys. Chem. B* **2004,** *108*, 9256-9263.
8. Gervais, C.; Dupree, R.; Pike, K. J.; Bonhomme, C.; Profeta, M.; Pickard, C. J.; Mauri, F., Combined First-Principles Computational and Experimental Multinuclear Solid-State NMR Investigation of Amino Acids. *J. Phys. Chem. A* **2005,** *109* (31), 6960-6969.
9. Peng, L.; Liu, Y.; Kim, N.; Readman, J. E.; Grey, C. P., Detection of Bronsted Acid Sites in Zeolite HY with High-Field 17O-MAS-NMR Techniques. *Nat. Mater.* **2005,** *4* (3), 216-219.
10. Ashbrook, S. E.; Smith, M. E., Solid state 17O NMR-An Introduction to the Background Principles and Applications to Inorganic Materials. *Chem Soc Rev* **2006,** *35* (8), 718-735.

11. van Beek, J. D.; Dupree, R.; Levitt, M. H., Symmetry-based Recoupling of 17O-1H Spin Pairs in Magic-Angle Spinning NMR. *J. Magn. Reson.* **2006,** *179* (1), 38-48.
12. Wong, A.; Pike, K. J.; Jenkins, R.; Clarkson, G. J.; Anupold, T.; Howes, A. P.; Crout, D. H.; Samoson, A.; Dupree, R.; Smith, M. E., Experimental and Theoretical 17O NMR Study of the Influence of Hydrogen-Bonding on C=O and O-H Oxygens in Carboxylic Solids. *J. Phys. Chem. A* **2006,** *110* (5), 1824-1835.
13. Hung, I.; Uldry, A. C.; Becker-Baldus, J.; Webber, A. L.; Wong, A.; Smith, M. E.; Joyce, S. A.; Yates, J. R.; Pickard, C. J.; Dupree, R.; Brown, S. P., Probing Heteronuclear 15N-17O and 13C-17O Connectivities and Proximities by Solid-State NMR Spectroscopy. *J. Am. Chem. Soc.* **2008,** *131*, 1820-1834.
14. Wu, G., Solid-state 17O NMR Studies of Organic and Biological Molecules. *Prog. Nucl. Magn. Reson. Spectrosc.* **2008,** *52* (2-3), 118-169.
15. Yamada, K., Recent Applications of Solid-State 17O NMR. *Annu. Rep. NMR Spectrosc.* **2010,** *70*, 115-158.
16. Huo, H.; Peng, L.; Grey, C. P., Measuring Brønsted Acid Site O–H Distances in Zeolites HY and HZSM-5 with Low-Temperature 17O–1H Double Resonance MAS NMR Spectroscopy. *J. Phys. Chem. C* **2011,** *115* (5), 2030-2037.
17. Kong, X.; O'Dell, L. A.; Terskikh, V.; Ye, E.; Wang, R.; Wu, G., Variable-Temperature 17O NMR Studies Allow Quantitative Evaluation of Molecular Dynamics in Organic Solids. *J. Am. Chem. Soc.* **2012,** *134* (35), 14609-14617.
18. Merle, N.; Trebosc, J.; Baudouin, A.; Rosal, I. D.; Maron, L.; Szeto, K.; Genelot, M.; Mortreux, A.; Taoufik, M.; Delevoye, L.; Gauvin, R. M., 17O NMR Gives Unprecedented Insights into the Structure of Supported Catalysts and their Interaction with the Silica Carrier. *J. Am. Chem. Soc.* **2012,** *134* (22), 9263-9275.
19. F. Blanc, L. Sperrin, D. A. Jefferson, S. Pawsey, M. Rosay, C. P. Grey, Dynamic Nuclear Polarization Enhanced Natural Abundance 17O Spectroscopy. *J. Am. Chem. Soc.* **2013,** *135* (8), 2975-2978.
20. Vogt, F. G.; Yin, H.; Forcino, R. G.; Wu, L., 17O Solid-State NMR as a Sensitive Probe of Hydrogen Bonding in Crystalline and Amorphous Solid Forms of Diflunisal. *Mol. Pharmaceutics* **2013,** *10* (9), 3433-3446.
21. Wang, M.; Wu, X. P.; Zheng, S.; Zhao, L.; Li, L.; Shen, L.; Gao, Y.; Xue, N.; Guo, X.; Huang, W.; Gan, Z.; Blanc, F.; Yu, Z.; Ke, X.; Ding, W.; Gong, X. Q.; Grey, C. P.; Peng, L., Identification of Different Oxygen Species in Oxide Nanostructures with 17O Solid-State NMR Spectroscopy. *Sci. Adv.* **2015,** *1* (1), e1400133.
22. Wu, G., Solid-State 17O NMR Studies of Organic and Biological Molecules: Recent Advances and Future Directions. *Solid State Nucl. Magn. Reson.* **2016,** *73*, 1-14.
23. Brownbill, N. J.; Gajan, D.; Lesage, A.; Emsley, L.; Blanc, F., Oxygen-17 Dynamic Nuclear Polarisation Enhanced Solid-State NMR Spectroscopy at 18.8 T. *Chem. Commun.* **2017,** *53* (17), 2563-2566.
24. Hope, M. A.; Halat, D. M.; Magusin, P. C.; Paul, S.; Peng, L.; Grey, C. P., Surface-Selective Direct 17O DNP NMR of CeO2 Nanoparticles. *Chem. Commun.* **2017,** *53* (13), 2142-2145.
25. Keeler, E. G.; Michaelis, V. K.; Colvin, M. T.; Hung, I.; Gor'kov, P. L.; Cross, T. A.; Gan, Z.; Griffin, R. G., 17O MAS NMR Correlation Spectroscopy at High Magnetic Fields. *J. Am. Chem. Soc.* **2017,** *139* (49), 17953–17963.

26. Perras, F. A.; Wang, Z.; Naik, P.; Slowing, I. I.; Pruski, M., Natural Abundance 17O DNP NMR Provides Precise O-H Distances and Insights into the Bronsted Acidity of Heterogeneous Catalysts. *Angew. Chem., Int. Ed.* **2017,** *56* (31), 9165-9169.
27. Gunawidjaja, P. N.; Holland, M. A.; Mountjoy, G.; Pickup, D. M.; Newport, R. J.; Smith, M. E., The Effects of Different Heat Treatment and Atmospheres on the NMR Signal and Structure of TiO2–ZrO2–SiO2 Sol–Gel Materials. *Solid State Nucl. Magn. Reson.* **2003,** *23* (1-2), 88-106.
28. Hampson, M. R.; Allen, S.; King, I. J.; Crossland, C. J.; Hodgkinson, P.; Harris, R. K.; Fayon, F.; Evans, J. S. O., Synthesis and NMR Studies of 17O Enriched AM2O8 Phases. *Solid State Sci.* **2005,** *7* (7), 819-826.
29. Seyfried, M. S.; Lauber, B. S.; Luedtke, N. W., Multiple-Turnover Isotopic Labeling of Fmoc- and Boc-Protected Amino Acids with Oxygen Isotopes. *Org. Lett.* **2010,** *12* (1), 104-6.
30. Theodorou, V.; Skobridis, K.; Alivertis, D.; Gerothanassis, I. P., Synthetic Methodologies in Organic Chemistry Involving Incorporation of 17O and 18O Isotopes. *J. Labelled Compd. Radiopharm.* **2014,** *57* (8), 481-508.
31. Metro, T. X.; Gervais, C.; Martinez, A.; Bonhomme, C.; Laurencin, D., Unleashing the Potential of 17O NMR Spectroscopy Using Mechanochemistry. *Angew. Chem., Int. Ed.* **2017,** *56* (24), 6803-6807.
32. Maly, T.; Debelouchina, G. T.; Bajaj, V. S.; Hu, K. N.; Joo, C. G.; Mak-Jurkauskas, M. L.; Sirigiri, J. R.; Wel, P. C. van der; Herzfeld, J.; Temkin, R. J.; Griffin, R. G., Dynamic Nuclear Polarization at High Magnetic Fields. *J. Chem. Phys.* **2008,** *128* (5), 052211.
33. Ni, Q. Z.; Daviso, E.; Can, T. V.; Markhasin, E.; Jawla, S. K.; Swager, T. M.; Temkin, R. J.; Herzfeld, J.; Griffin, R. G., High Frequency Dynamic Nuclear Polarization. *Acc. Chem. Res.* **2013,** *46* (9), 1933-1941.
34. Michaelis, V. K.; Ong, T. C.; Kiesewetter, M. K.; Frantz, D. K.; Walish, J. J.; Ravera, E.; Luchinat, C.; Swager, T. M.; Griffin, R. G., Topical Developments in High-Field Dynamic Nuclear Polarization. *Isr. J. Chem.* **2014,** *54* (1-2), 207-221.
35. Perras, F. A.; Kobayashi, T.; Pruski, M., Natural Abundance 17O DNP Two-Dimensional and Surface-Enhanced NMR Spectroscopy. *J. Am. Chem. Soc.* **2015,** *137* (26), 8336-8339.
36. Perras, F. A.; Chaudhary, U.; Slowing, I. I.; Pruski, M., Probing Surface Hydrogen Bonding and Dynamics by Natural Abundance, Multidimensional, 17O DNP-NMR Spectroscopy. *J. Phys. Chem. C* **2016,** *120* (21), 11535-11544.
37. Kong, X.; Dai, Y.; Wu, G., Solid-state 17O NMR Study of 2-Acylbenzoic Acids and Warfarin. *Solid State Nucl. Magn. Reson.* **2017,** *84*, 59-64.
38. Chekmenev, E. Y.; Waddell, K. W.; Hu, J.; Gan, Z.; Wittebort, R. J.; Cross, T. A., Ion-Binding Study by 17O Solid-State NMR Spectroscopy in the Model Peptide Gly-Gly-Gly at 19.6 T. *J. Am. Chem. Soc.* **2006,** *128* (30), 9849-9855.
39. Jakobsen, H. J.; Bildsøe, H.; Brorson, M.; Wu, G.; Gor'kov, P. L.; Gan, Z.; Hung, I., High-Field 17O MAS NMR Reveals 1J(17O-127I) with its Sign and the NMR Crystallography of the Scheelite Structures for NaIO4and KIO4. *J. Phys. Chem. C* **2015**, 14434-14442.
40. Wu, G.; Rovnyank, D.; Sun, B.; Griffin, R., High-Resolution Multiple Quantum MAS NMR Spectroscopy of Half-Integer Quadrupolar Nuclei. *Chem. Phys. Lett.* **1995,** (249), 210-217.
41. Xu, Z.; Maekawa, H.; Oglesby, J. V.; Stebbins, J. F., Oxygen Speciation in Hydrous Silicate Glasses: An Oxygen-17 NMR Study. *J. Am. Chem. Soc.* **1998,** *120* (38), 9894-9901.

42. Cavadini, S.; Antonijevic, S.; Lupulescu, A.; Bodenhausen, G., Indirect detection of nitrogen-14 in solid-state NMR spectroscopy. *ChemPhysChem* **2007,** *8* (9), 1363-74.
43. Vega, A. J., CP/MAS of Quadrupolar S = 3/2 Nuclei. *Solid State Nucl. Magn. Reson.* **1992,** *1* (1), 17-32.
44. Vega, A. J., Mas NMR Spin Locking of Half-Integer Quadrupolar Nuclei. *J. Magn. Reson.* **1992,** *96* (1), 50-68.
45. Amoureux, J. P.; Pruski, M., Theoretical and Experimental Assessment of Single- and Multiple-Quantum Cross-Polarization in Solid State NMR. *Mol. Phys.* **2002,** *100* (10), 1595-1613.
46. Amoureux, J. P.; Trebosc, J.; Wiench, J.; Pruski, M., HMQC and Refocused-INEPT Experiments Involving Half-Integer Quadrupolar Nuclei in Solids. *J. Magn. Reson.* **2007,** *184* (1), 1-14.
47. Venkatesh, A.; Hanrahan, M. P.; Rossini, A. J., Proton Detection of MAS Solid-State NMR Spectra of Half-Integer Quadrupolar Nuclei. *Solid State Nucl. Magn. Reson.* **2017,** *84*, 171-181.
48. Yao, Z.; Kwak, H. T.; Sakellariou, D.; Emsley, L.; Grandinetti, P. J., Sensitivity Enhancement of the Central Transition NMR Signal of Quadrupolar Nuclei Under Magic-Angle Spinning. *Chem. Phys. Lett.* **2000,** *327* (1-2), 85-90.
49. Steinchneider, A.; Burgar, M. I.; Buku, A.; Fiat, D., Labeling of Amino Acids and Peptides with Isotopic Oxygen as Followed by 17O-NMR. *Int. J. Pept. Protein Res.* **1981,** *18*, 324-333.
50. Larsen, F. H.; Jakobsen, H. J.; Ellis, P. D.; Nielsen, N. C., QCPMG-MAS NMR of Half-Integer Quadrupolar Nuclei. *J. Magn. Reson.* **1998,** *131* (1), 144-7.
51. Zhao, X.; Sudmeier, J. L.; Bachovchin, W. W.; Levitt, M. H., Measurement of NH Bond Lengths by Fast Magic-Angle Spinning Solid-State NMR Spectroscopy: A New Method for the Quantification of Hydrogen Bonds. *J. Am. Chem. Soc.* **2001,** *123* (44), 11097-8.
52. Zhao, X.; Hoffbauer, W.; Gunne, J. Schmedt auf der; Levitt, M. H., Heteronuclear Polarization Transfer by Symmetry-Based Recoupling Sequences in Solid-State NMR. *Solid State Nucl. Magn. Reson.* **2004,** *26* (2), 57-64.
53. Brinkmann, A.; Kentgens, A. P., Proton-Selective 17O-1H Distance Measurements in Fast Magic-Angle-Spinning Solid-State NMR Spectroscopy for the Determination of Hydrogen Bond Lengths. *J. Am. Chem. Soc.* **2006,** *128* (46), 14758-14759.
54. Brinkmann, A.; Kentgens, A. P., Sensitivity Enhancement and Heteronuclear Distance Measurements in Biological 17O Solid-State NMR. *J. Phys. Chem. B* **2006,** *110* (32), 16089-16101.
55. Case, D. A., Calculations of NMR Dipolar Coupling Strengths in Model Peptides. *J. Biomol. NMR* **1999,** *15* (2), 95-102.
56. Yamada, K.; Hashizume, D.; Shimizu, T.; Ohki, S.; Yokoyama, S., A Solid-State 17O NMR, X-ray, and Quantum Chemical Study of N-α-Fmoc-Protected Amino Acids. *J. Mol. Struct.* **2008,** *888* (1-3), 187-196.
57. Peterson, S. W.; Levy, Henri A., Structure of Potassium Hydrogen Maleate by Neutron Diffraction. *J. Chem. Phys.* **1958,** *29* (4), 948-949.
58. Lehmann, M. S.; Koetzle, T. F.; Hamilton, W. C., Precision Neutron Diffraction Structure Determination of Protein and Nucleic Acid Components. I. The Crystal and Molecular Structure of the Amino Acid L-Alanine. *J. Am. Chem. Soc.* **1972,** *94* (8), 2657-60.

59. Deringer, V. L.; Hoepfner, V.; Dronskowski, R., Accurate Hydrogen Positions in Organic Crystals: Assessing a Quantum-Chemical Aide. *Cryst. Growth Des.* **2012,** *12* (2), 1014-1021.
60. Pople, J. A., The Effect of Quadrupole Relaxation on Nuclear Magnetic Resonance Multiplets. *Mol. Phys.* **1958,** *1* (2), 168-174.
61. Burnett, L. J.; Zeltmann, A. H., 1H–17O Spin- Spin Coupling Constant in Liquid Water. *J. Chem. Phys.* **1974,** *60* (11), 4636-4637.
62. Versmold, H.; Yoon, C., Oxygen-17 NMR Studies of Methanol and Ethanol. *Ber. Bunsen-Ges.* **1972,** *76* (11), 1164-1168.
63. Bolkunov, I. A.; Sergeyev, N. M., 17O, 1H Coupling Constants in Intramolecular Hydrogen Bonds. *Chem. Phys. Lett.* **1990,** *174* (6), 587-590.
64. Sutter, K.; Aucar, G. A.; Autschbach, J., Analysis of Proton NMR in Hydrogen Bonds in Terms of Lone-Pair and Bond Orbital Contributions. *Chem. Eur. J.* **2015,** *21* (50), 18138-55.
65. Duma, L.; Lai, W. C.; Carravetta, M.; Emsley, L.; Brown, S. P.; Levitt, M. H., Principles of Spin-Echo Modulation by J-Couplings in Magic-Angle-Spinning Solid-State NMR. *ChemPhysChem* **2004,** *5* (6), 815-833.
66. Trébosc, J.; Amoureux, J. P.; Delevoye, L.; Wiench, J. W.; Pruski, M., Frequency-Selective Measurement of Heteronuclear Scalar Couplings in Solid-State NMR. *Solid State Sci.* **2004,** *6* (10), 1089-1095.
67. Amoureux, J. P.; Trebosc, J.; Wiench, J. W.; Massiot, D.; Pruski, M., Measurement of J-Couplings Between Spin-(1/2) and Quadrupolar Nuclei by Frequency Selective Solid-State NMR. *Solid State Nucl Magn Reson* **2005,** *27* (4), 228-32.
68. Penzel, S.; Smith, A. A.; Ernst, M.; Meier, B. H., Setting the Magic Angle for Fast Magic-Angle Spinning Probes. *J. Magn. Reson.* **2018,** *293*, 115-122.
69. Antonijevic, S.; Bodenhausen, G., High-Resolution NMR Spectroscopy in Solids by Truly Magic-Angle Spinning. *Angew. Chem., Int. Ed.* **2005,** *44* (19), 2935-2938.
70. Ernst, M.; Verhoeven, A.; Meier, B. H., High-Speed Magic-Angle Spinning 13C MAS NMR Spectra of Adamantane: Self-Decoupling of the Heteronuclear Sscalar Interaction and Proton Spin Diffusion. *J. Magn. Reson.* **1998,** *130* (2), 176-85.
71. Lesage, A.; Steuernagel, S.; Emsley, L., Carbon-13 Spectral Editing in Solid-State NMR using Heteronuclear Scalar Couplings. *J. Am. Chem. Soc.* **1998,** *120* (28), 7095-7100.
72. Ernst, M.; Meier, B. H., *Studies in Physical and Theoretical Chemistry*. 1998; Vol. 84.
73. Nyfeler, D.; Armbruster, T., Silanol Groups in Minerals and Inorganic Compounds. *Am. Mineral.* **1998,** *83* (1-2), 119-125.
74. Bucko, T.; Benco, L.; Demuth, Th.; Hafner, J., Ab Initio Density Functional Investigation of the (001) Surface of Mordenite. *J. Chem. Phys.* **2002,** *117* (15), 7295-7305.
75. Hartman, J. D.; Kudla, R. A.; Day, G. M.; Mueller, L. J.; Beran, G. J., Benchmark Fragment-Based 1H, 13C, 15N and 17O Chemical Shift Predictions in Molecular Crystals. *Phys. Chem. Chem. Phys.* **2016,** *18* (31), 21686-709.
76. Kobayashi, T.; DiVerdi, J. A.; Maciel, G. E., Silica gel surface: Molecular dynamics of surface silanols. *J. Phys. Chem. C* **2008,** *112* (11), 4315-4326.
77. Ashbrook, S. E.; McKay, D., Combining Solid-State NMR Spectroscopy with First-Principles Calculations - A Guide to NMR Crystallography. *Chem. Commun.* **2016,** *52* (45), 7186-7204.
78. Wilkens, S. J.; Westler, W. M.; Markley, J. L.; Weinhold, F., Natural J-Coupling Analysis: Interpretation of Scalar J-Couplings in Terms of Natural Bond Orbitals. *J. Am. Chem. Soc.* **2001,** *123* (48), 12026-12036.

79. Czernek, J.; Bruschweiler, R., Geometric Dependence of 3hJ(31P-15N) and 2hJ(31P-1H) Scalar Couplings in Protein-Nucleotide Complexes. *J. Am. Chem. Soc.* **2001,** *123*, 11079-11080.
80. Salvador, P.; Wieczorek, R.; Dannenberg, J. J., Direct Calculation of trans-Hydrogen-Bond 13C-15N 3-Bond J-Couplings in Entire Polyalanine r-Helices. A Density Functional Theory Study. *J. Phys. Chem. B* **2007,** *111*, 2398-2403.